

YMTHE, Volume 25

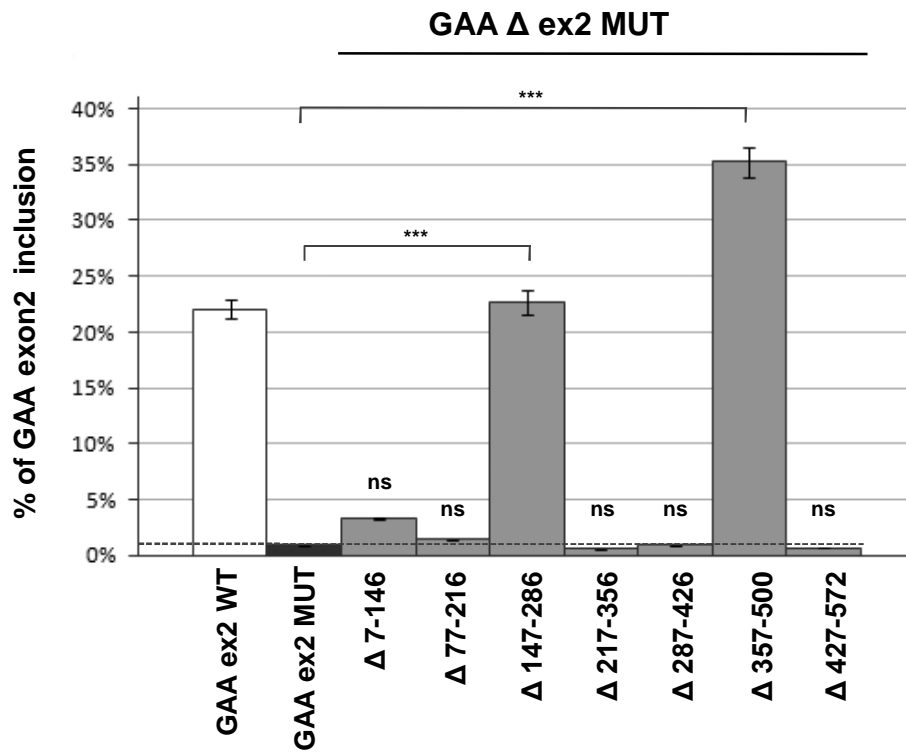
Supplemental Information

**Glycogen Reduction in Myotubes
of Late-Onset Pompe Disease Patients
Using Antisense Technology**

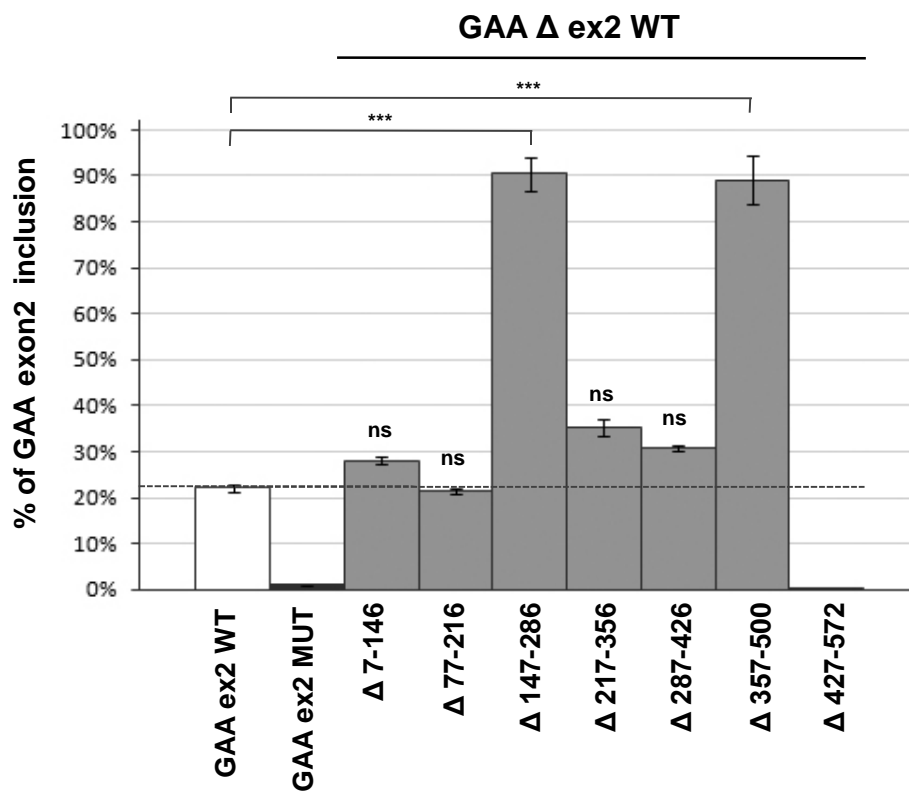
Elisa Goina, Paolo Peruzzo, Bruno Bembi, Andrea Dardis, and Emanuele Buratti

Figure S1.

a



b



c

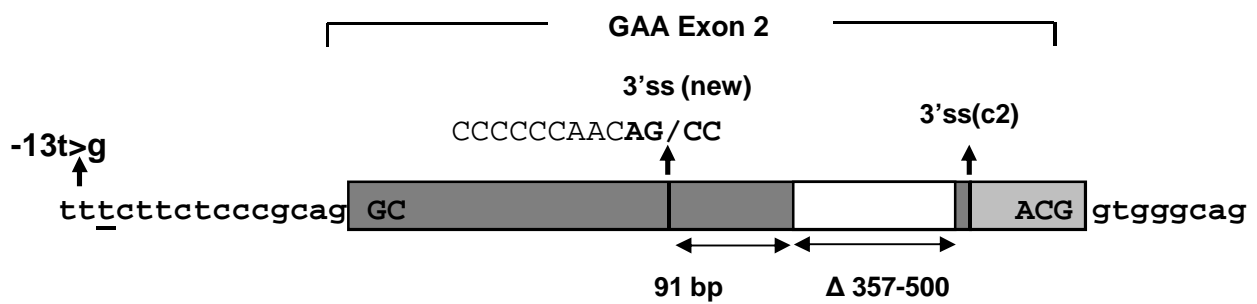


Figure S3.

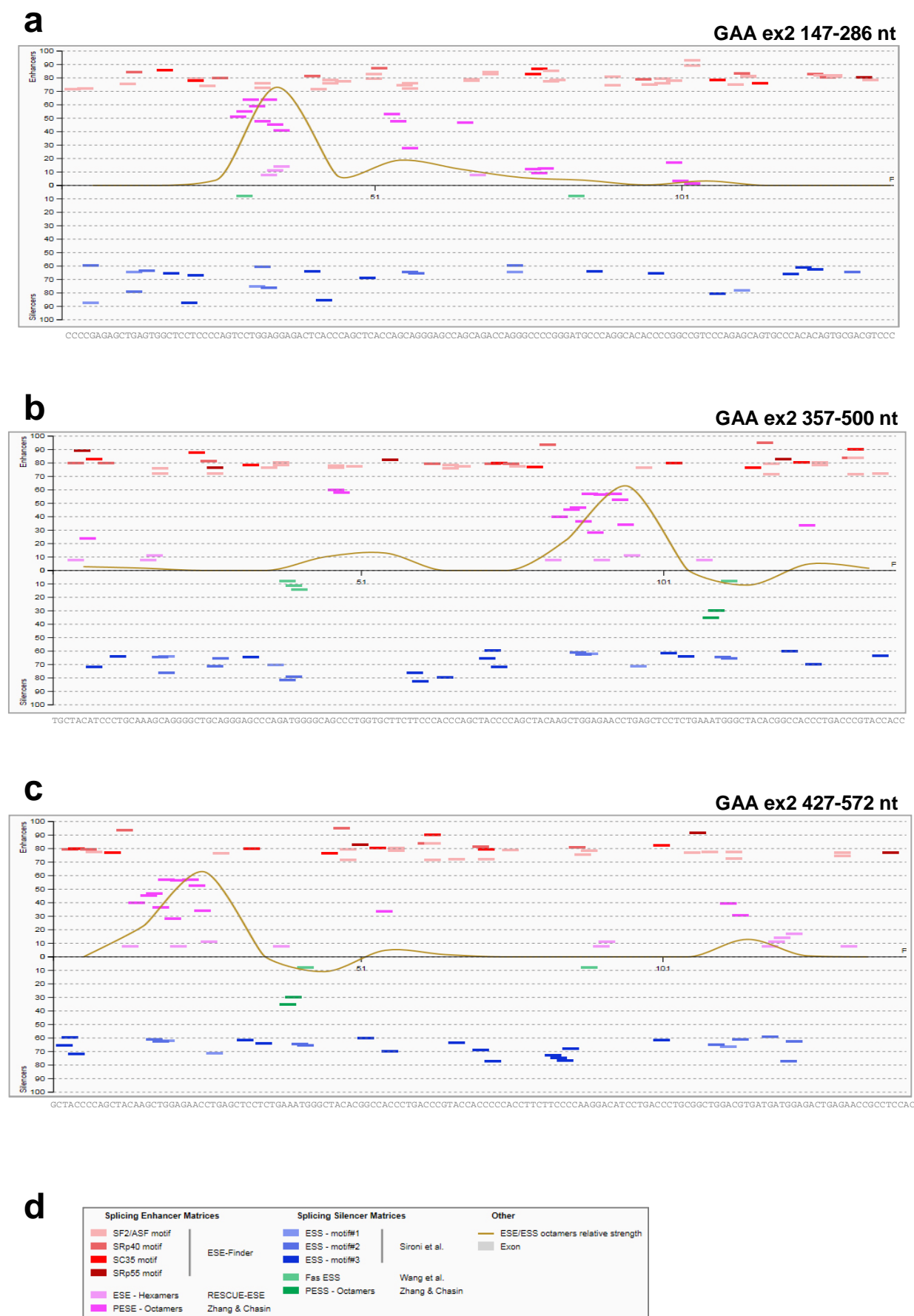
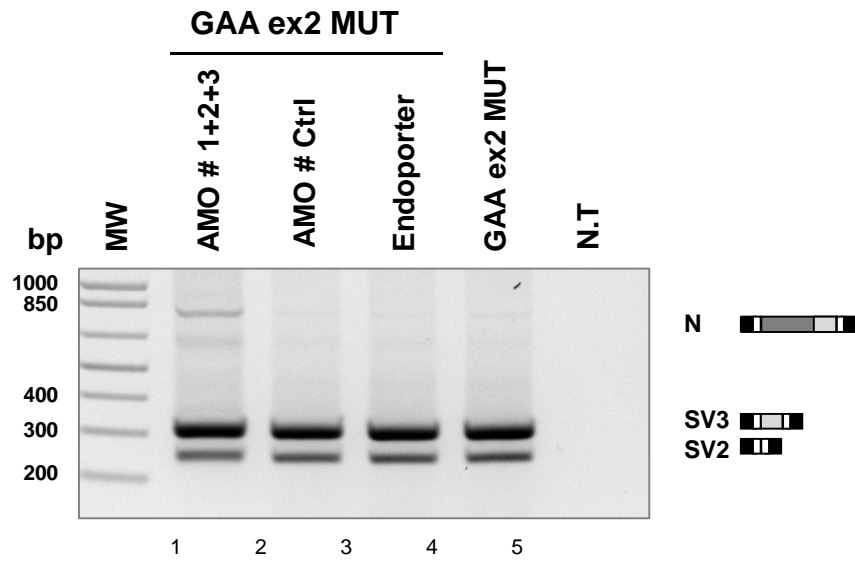


Figure S4.

a



b

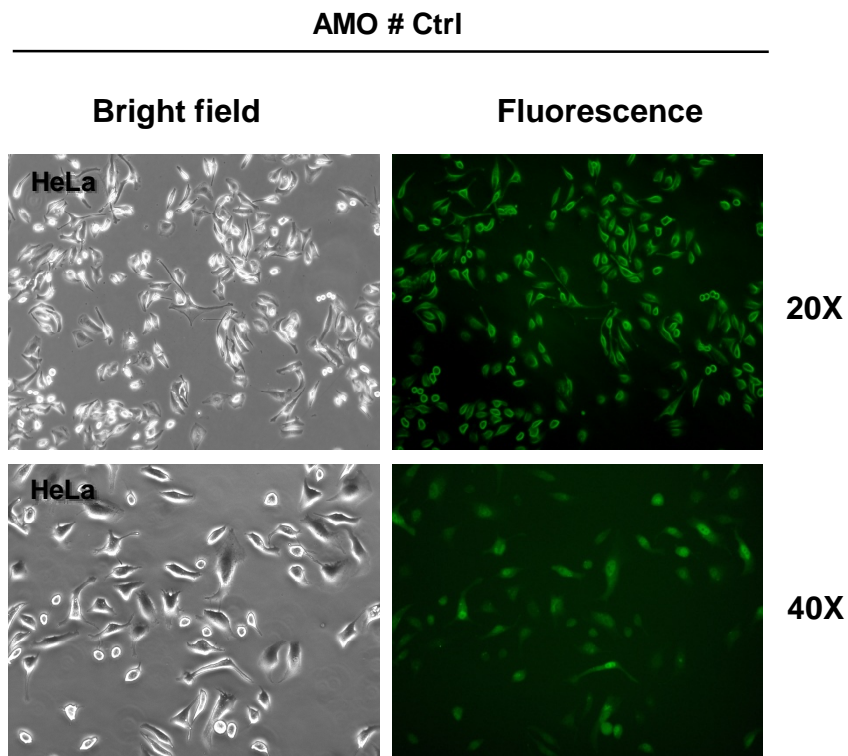
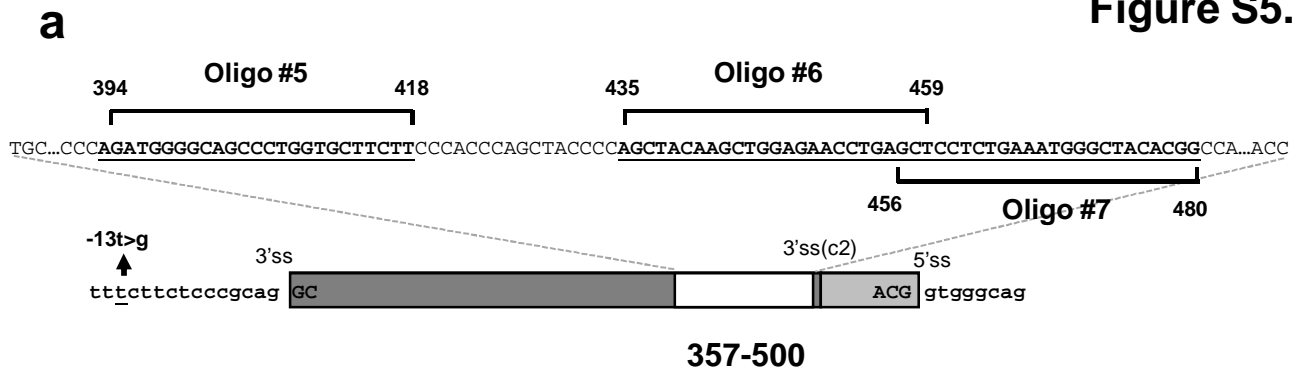
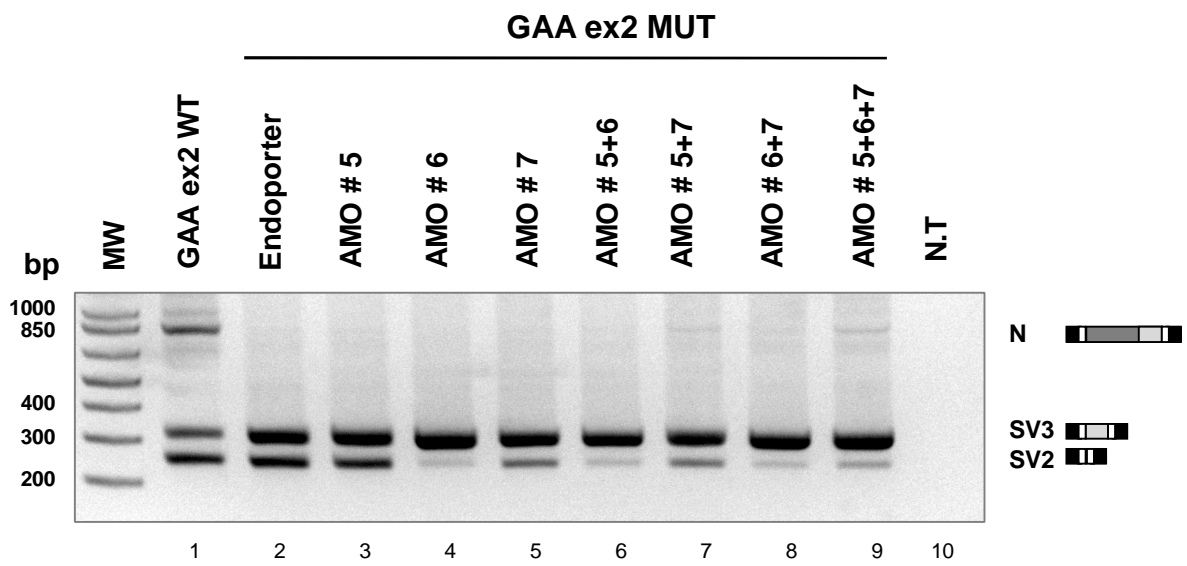


Figure S5.



b



c

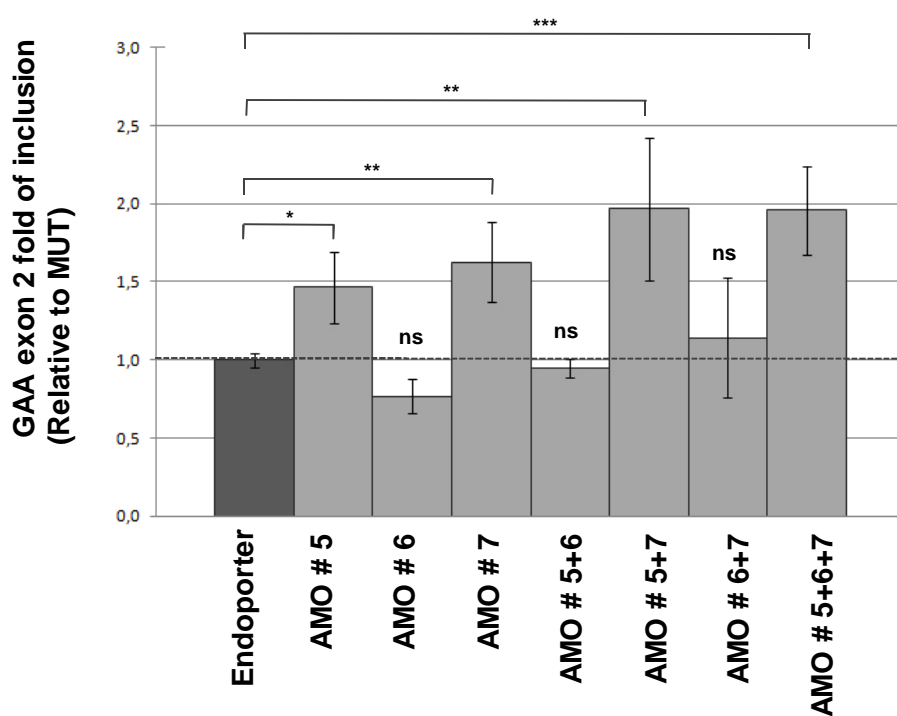
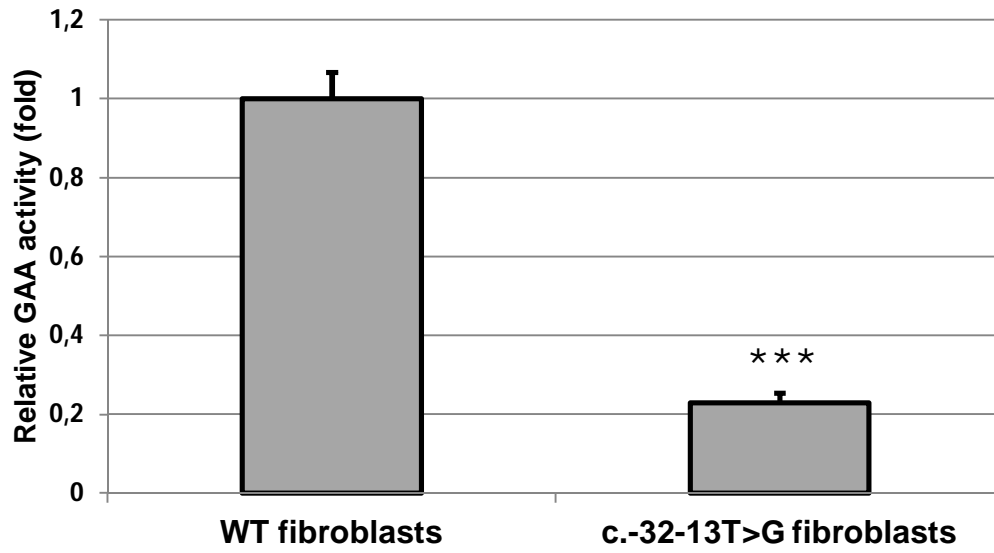


Figure S6.

a



b

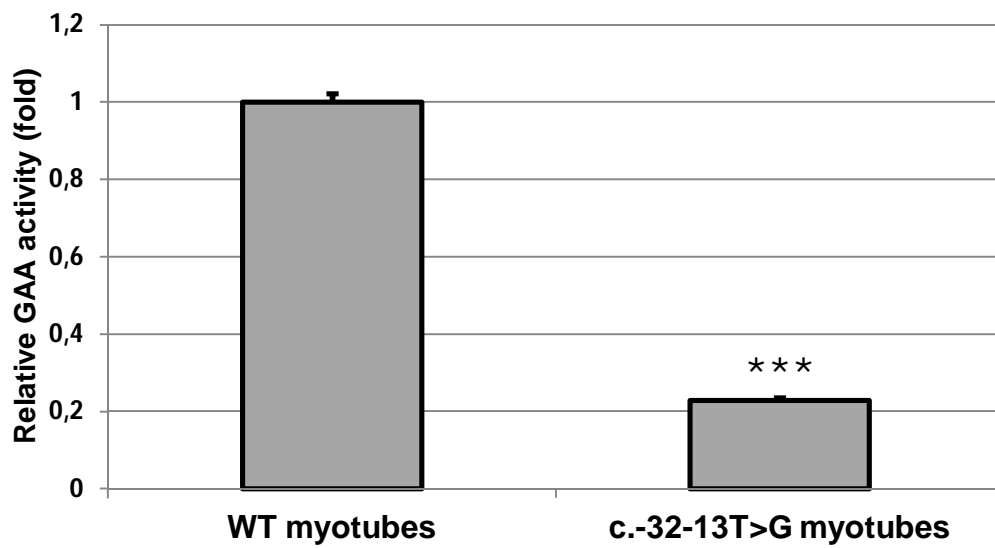
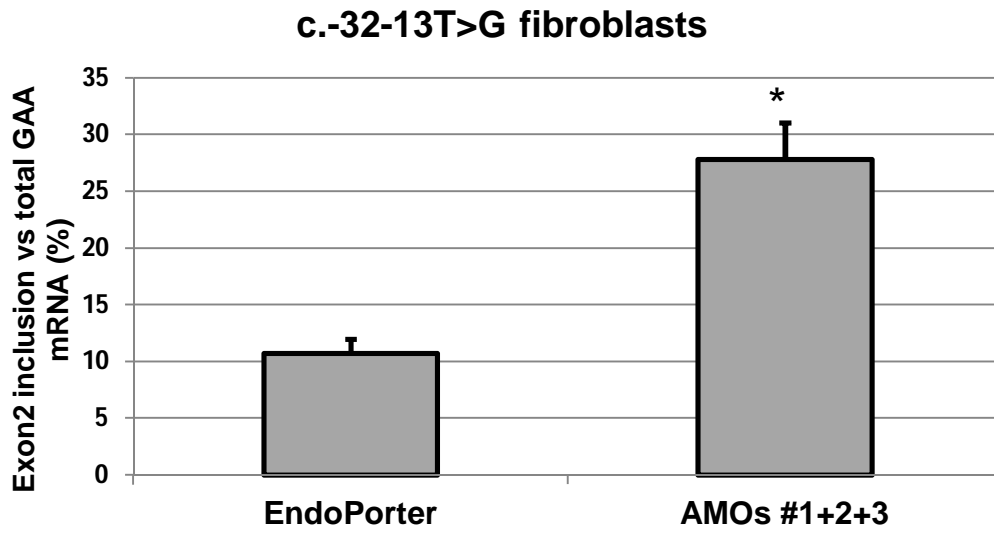
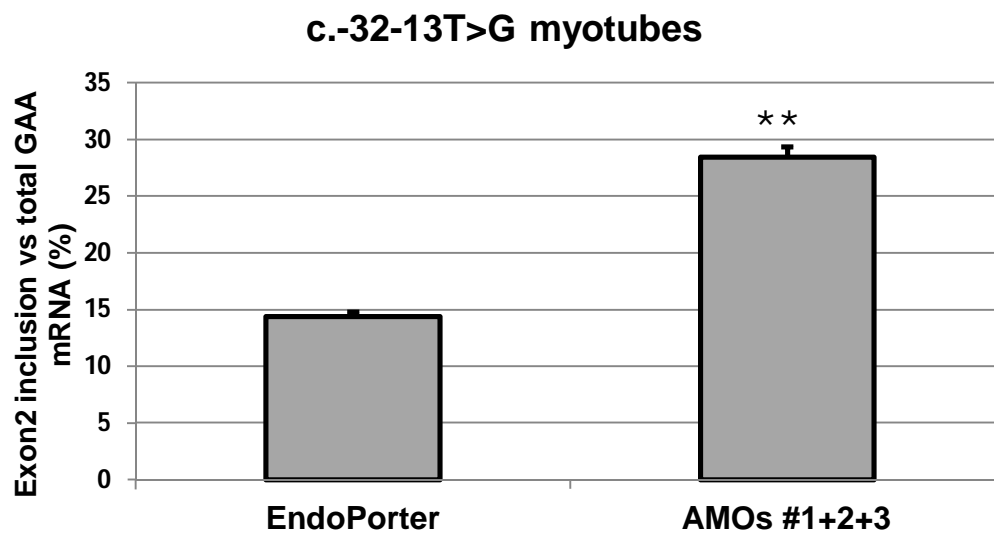


Figure S7.

a



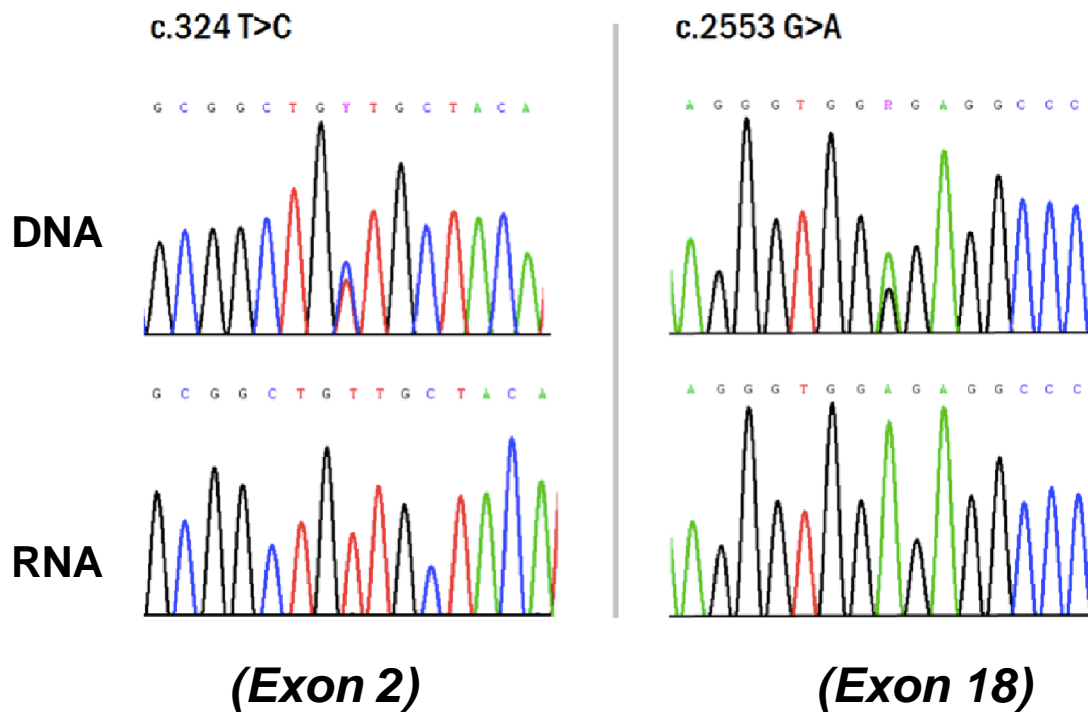
b



a

LO-GSDII myoblasts

Genotype: c.-32-13T>G; c.2646_2646+1delTG



SUPPLEMENTARY FIGURE LEGENDS.

Supplementary Figure 1. Quantification of *GAA* exon 2 inclusion in HeLa transfected with *GAA* delta exon 2 MUT and WT minigenes. (a-b) Graphical representation of the quantification of the intensity of the bands corresponding to the *GAA* exon 2 (N) generated after transfection of *GAA* delta exon 2 MUT and WT minigenes. The intensity of the bands analyzed by ImageJ and expressed as a percentage. Data are represented as means \pm SD of three independent experiments ($***P < 0.001$). (c) Schematic illustration of the $\Delta 357-500$ minigene and the position of the new activated cryptic 3' splice sites. The new 3' splice sites are located 91 nt upstream the $\Delta 357-500$ region. The identity of the band was confirmed by sequencing.

Supplementary Figure 2. Screening of SFRS proteins able to bind *GAA* exon 2 by Western Blot analysis. (a) Western blot analysis after pull down assay using specific antibodies against SFRSs. The nuclear extract sample (NE) corresponds to 1/20th of the total amount of protein used for the pull down assay. The western blot pictures show representative results of three independent experiments. Empty beads were used as a control (Beads). (b-d) Analysis performed by the bioinformatic tool SpliceAid2. Graphical representation of the putative binding sites for splicing factors within the 147-286 nt (b), to 357-500 nt (c) and to 427-572 nt (d) regions of *GAA* exon 2. Positive scores were assigned to target sequences classified as exonic splicing enhancer motifs whereas negative scores to exonic splicing silencer motifs. The height and the width of the bars correlate with the binding affinity and the number of nucleotides encompassing the binding site, respectively. The splicing factor name predicted to bind each sequence is indicated on top of each bar.

Supplementary Figure 3. Analysis performed using the bioinformatic tool Human Splicing Finder 3. (a-c) Graphical representation of putative exonic regulatory regions within the 147-286 nt (a), to 357-500 nt (b) and to 427-572 nt (c) *GAA* exon 2 sequences. The position of exonic splicing enhancer motifs is shown in the upper part of each graph whereas exonic splicing silencer motifs are reported in the lower part. (d) Each colour corresponds to a different prediction algorithm as

described in the panel d.

Supplementary Figure 4. Control AMO transfection does not affect splicing pattern of *GAA* ex2 MUT minigene. (a) RT-PCR analysis of HeLa cells co-transfected with AMOs #1,2 and 3 to a final concentration of 15 μ M and the *GAA* ex2 MUT minigene. Control AMO was delivered to a final concentration of 10 μ M together with the *GAA* ex2 MUT minigene. Cells transfected with the MUT minigene together with EndoPorter reagent and MUT minigene alone were used as internal control; not transfected cells (N.T.) were used as RT-PCR control. The agarose gel picture shows a representative result of three independent experiments. (b) Fluorescence distribution to confirm control AMO delivery. Brightfield and fluorescence images at 20X and 40X magnification show the uptake of the control AMO fluorescently labeled in HeLa cells 48h after transfection. Cells show normal morphology and diffuse fluorescence distribution.

Supplementary Figure 5. Effect of AMOs against region 357-500 on exon 2 inclusion in the MUT minigene context. (a) Schematic representation of AMOs #5, 6 and 7 targeting the 357-500 region of *GAA* exon 2. The AMOs target sequences are indicated by black lines. (b) RT-PCR analysis of HeLa cells co-transfected with AMOs #5,6 and 7 and the *GAA* ex2 MUT minigene. AMOs were delivered as single unit or in different combination to a final concentration of 15 μ M. Cells transfected with the mutated minigene together with EndoPorter reagent were used as internal control; not transfected cells (N.T.) were used as RT-PCR control. The agarose gel picture shows a representative result of three independent experiments. (c) RT-qPCR analysis of *GAA* exon 2 inclusion (N) in cells co-transfected with AMOs (#5+6+7) and the *GAA* MUT minigene. The relative abundance of N form is expressed as fold of increase over the *GAA* ex2 MUT minigene alone. RT-qPCR data are represented as means \pm SEM of three independent experiments in a histogram plot (* P < 0.05; ** P < 0.01; *** P < 0.001).

Supplementary Figure 6. *GAA* enzymatic activity in cultured fibroblasts and myotubes. *GAA* enzymatic activity in cultured fibroblasts (a) and myotubes (b) from a normal control (WT) and a

patient carrying the c.-32-13T>G mutation. Data are expressed as percentage of WT activity and represent the mean \pm SEM of three independent experiments (*** = $p < 0,001$; t-test statistics).

Supplementary Figure 7. Effect of AMOs targeting the 147-286 region on absolute percentage of exon 2 inclusion in patient's cells.

Exon 2 inclusion expressed as percentage of total *GAA* mRNA in c-32-13T>G fibroblasts (a) and myotubes (b) before and after 48h treatment with AMOs 1+2+3. The amount of exon 2 inclusion (N form) was analyzed using primers that specifically amplified mRNA containing exon 2 while the total amount of *GAA* transcript was determined using primers that target a region spanning *GAA* exon 18-19. Data are expressed as mean \pm SEM of at least two independent experiments (* = $p < 0,05$; ** = $p < 0,01$; t-test statistics).

Supplementary Figure 8. Genomic DNA and mRNA Sanger sequencing of LO-GSDII myoblasts carrying the c.-32-13T>G and the c.2646_2646+1delTG mutations in the *GAA* gene.

(a) Electropherogram results showing two single nucleotide polymorphisms (c.324T>C in exon 2 and c.2553G>A in exon 18) that were found at the DNA but not at the mRNA level, indicating that only one *GAA* allele was expressed in these LO-GSDII myoblasts.

Table S1.

Primers for inserting deletions in pTB GAA Wt and MUT minigenes:

Δ7-146Fw	5'-tgagcccgctttcttctcccgcagGCCTGTCCCCGAGAGCTGAGTGGCTCCTC CCCAGTC-3'
Δ7-146Rv	5'-GACTGGGGAGGAGCCACTCAGCTCTCGGGGACAGGCctgcgggagaa gcaagcgggctca-3'
Δ77-216Fw	5'-CCCGCCCTGCTCCCACCGGCTCCTGGCCGTGACCAGGGCCCCGG GATGCCCAGGCACACC-3'
Δ77-216Rv	5'-GGTGTGCCTGGGCATCCCGGGGCCCTGGTCACGGCCAGGAGCCG GTGGGAGCAGGGCGGG-3'
Δ147-286Fw	5'-ACATCCTACTCCATGATTTCTGCTGGTTCCCCAACAGCCGCTTCG ATTGCGCCCCTG-3'
Δ147-286Rv	5'-CAGGGGCGCAATCGAAGCGGCTGTTGGGGAACCAGCAGGAAATC ATGGAGTAGGATGT-3'
Δ217-356Fw	5'-CTCACCCAGCTCACCAGCAGGGAGCCAGCATGCTACATCCCTGCA AAGCAGGGGCTGCAG-3'
Δ217-356Rw	5'-CTGCAGCCCCTGCTTTGCAGGGATGTAGCATGCTGGCTCCCTGCT GGTGAGCTGGGTGAG-3'
Δ287-426Fw	5'-CAGAGCAGTGCCACACAGTGCGACGTCCCGCTACCCAGCTACA AGCTGGAGAACCTGA-3'
Δ287-426Rw	5'-TCAGGTTCTCCAGCTTGTAGCTGGGGTAGCGGGACGTCGCACTGT GTGGGCACTGCTCTG-3'
Δ357-500Fw	5'-ACCCAGGAACAGTGCGAGGCCCGCGGCTGTCCCACCTTCTTCCC AAGGACATCCTGACC-3'
Δ357-500Rw	5'-GGTCAGGATGTCCTTGGGGAAGAAGGTGGGACAGCCGCGGGCCT CGCACTGTTCTTGGGT-3'
Δ427-572Fw	5'-TGGGGCAGCCCTGGTGCTTCTTCCCACCCATTCACGgtgggcagggcag gggcggggcg-3'
Δ427-572Rv	5'-cgccccgcccctgcctgcccacCGTGAATGGGTGGGAAGAAGCACCAGG GCTGCCCCA-3'

Primer for inserting the single mutation -13T/G:

hGAA-13Gs	5'-GAGCCCGCTTGCTTCTCCCGC-3'
hGAA-13Gas	5'-GCGGGAGAAGCAAGCGGGCTC-3'

Primer for end-point PCR on GAA cDNA after AMOs treatment:

GAA Fw	5'-CCACCTCTAGGTTCTCCTCGT-3'
SKIP2 Rv	5'-CGGAGAACTCCACGCTGTA-3'

Primers for RT-PCR:

GLO 800Bis Rv	5'-CACAGAAGCCAGGAACTTGTCC-3'
Alfa 2-3 Fw	5'-CAACTTCAAGCTCCTAAGCCACTGC-3'
BRA 2 Rv	5'-TAGGATCCGGTCACCAGGAAGTTGGTTAAATCA-3'

Oligo morpholino:

Oligo #1 (199-223)	5'-CCTGGTCTGCTGGCTCCCTGCTGGT-3'
Oligo #2 (230-254)*	5'-ACG <u>a</u> CCGGGGTGTGCCTG <u>a</u> GCATCC-3'
Oligo #3 (258-282)	5'-CGTCGCACTGTGTGGGCACTGCTCT-3'
Oligo #5 (394-418)	5'-AAGAAGCACCAGGGCTGCCCCATCT-3'
Oligo #6 (435-459)	5'-AGCTCAGGTTCTCCAGCTTGTAGCT-3'
Oligo #7 (456-480)	5'-CCGTGTAGCCCATTTCAGAGGAGCT-3'

*Morpholino #2 (230-254) carries two point mutation (underlined letters) to avoid strong secondary structure, without compromising its binding to the target sequence.

Primers for RealTime PCR:

GAA F3 Fw	5'-CCCGGCCTGGAGTACAATG-3'
GAA R3 Rv	5'-CAGGAGTGCAGCGGTTGC-3'
AlfaGlo2 142 Fw	5'-ACCAAGACCTACTTCCCGCACTTCG-3'
AlfaGlo2-3 294 Rv	5'-CAGGCAGTGGCTTAGGAGCTTGAAG-3'
GAA ex1-2 Fw	5'-CCACCTCTAGGTTCTCCTCGT-3'
GAA ex1-2 Rv	5'-TCCTACAGGCCCGCTCC-3'
GAA ex18-19 Fw	5'-GAGCTGTTCTGGGACGATG-3'
GAA ex18-19 Rv	5'-GCAGCTGCAGGCCAGCTCC-3'
HPRT Fw	5'-GACCAGTCAACAGGGGACAT-3'
HPRT Rv	5'-GTGTCAATTATATCTTCCACAATCAAG-3'

Primers for Pulldown:

T7 147-286 Fw	5'-TAATACGACTCACTATAGGGCCCCGAGAGCTGAGTGGCTC-3'
147-286 Rv	5'-GGGACGTCGCACTGTGTGGGCAC-3'
T7 357-500 Fw	5'-TAATACGACTCACTATAGGGTGCTACATCCCTGCAAAGCA-3'
357-500 Rv	5'-GGTGGTACGGGTCAGGGTGGCCGTG-3'
T7 427-571 Fw	5'-TAATACGACTCACTATAGGGGCTACCCAGCTACAAGCTG-3'
427-571 Rv	5'-TGGAGGCGGTTCTCAGTCTCCATC-3'

Table S2. Normality test (Shapiro-Wilk). *p*-values >0.05 indicate a normal distribution.

HeLa cells co-transfected with AMOs #1, 2 and 3 and the *GAA* MUT minigene (Fig. 3c).

Dataset	W	n	<i>p</i>-values
Endopporter	0.938340	10	0.534700
AMO #1	0.824235	8	0.051689
AMO #2	0.994243	4	0.978066
AMO #3	0.839796	4	0.194808
AMO #1+2	0.769482	4	0.057806
AMO #1+3	0.918227	4	0.527055
AMO #2+3	0.788121	4	0.082567
AMO #1+2+3	0.943869	6	0.690506

HeLa cells co-transfected with AMOs #5, 6 and 7 and the *GAA* MUT minigene (Fig. S5c).

Dataset	W	n	<i>p</i>-values
Endopporter	0.946550	9	0.652269
AMO #5	0.897723	5	0.397426
AMO #6	0.773414	3	0.052494
AMO #7	0.855847	3	0.256216
AMO # 5+6	0.855684	5	0.213163
AMO # 5+7	0.772879	3	0.051274
AMO # 6+7	0.830194	3	0.188826
AMO # 5+6+7	0.927684	7	0.531376

Patient fibroblasts transfected with AMOs #1, 2 and 3 (Fig. 4b).

Dataset	W	n	<i>p</i>-values
Endopporter	0.854651	3	0.252970
AMO #1	0.779125	3	0.065581
AMO #2	0.919708	3	0.451310
AMO #3	0.979908	3	0.728367
AMO #1+2+3	0.935960	3	0.511376